INDUCTION MOTOR: A NEW STATIC ODEL

Luis AROMATARIS Fabian RINAUDO Juan ALEMANY Marcos GALETTO
Universidad Nacional de Río Cuarto, Rio Cuarto (Cba), Argentina
Ruta 36 km 601, Phone: 543584676495, laromata@ing.unrc.edu.ar

Abstract: *Voltage stability in power system is largely determined by the characteristics of the load. In order to obtain reliable results in voltage stability, the load model must be represented as realistically as possible. The issue is even more challenging with static voltage stability techniques, because dynamic loads must be represented by static models. The commonly used static models are constant impedance, constant current, and constant power. A significant part of the load is made up of induction motors that are usually modeled as static constant power loads. Under variations of terminal voltage of the motor, this static model can approximately represent the active power, but it can commit major mistakes when representing the behavior of reactive power. Therefore, a new motor static model will be developed in this work.*

Key words: *Induction motor, Voltage Stability, Load model, Static Techniques*

1. Introduction

It has been widely recognized that electrical loads have a significant impact on dynamic performances of the wide area power system, and that accurate load models are highly important for power system dynamic simulation and analysis [1]. Hence their behavior has crucial impacts on power system dynamic behavior, especially voltage stability and voltage performance [2]. Specifically, voltage stability analysis and simulation results are greatly affected by the use of different load models [3, 8]. In order to obtain reliable results when studying this problem with numerical simulations, the chosen model to represent the load must represent behavior as realistically as possible. The need for accurate modeling of loads has risen as a result of a number of blackouts that have taken place worldwide [3]. The induction motor loads that are considered dynamic loads account for a great amount of electric loads, especially in large industries and air-conditioning of commercial and residential areas [4].

The modeling issue is even more challenging with static voltage stability techniques [14] because loads with dynamic behavior must be represented by static models. Static loads are represented by algebraic equations using an exponential model, which depends on the load terminal voltage. The commonly used models are referred to as: constant impedance, constant current, constant power, zip model or exponential model [9].

In conventional static voltage stability studies [6, 7, 10], constant impedance and constant current models are considered as allowing the simulation of a large amount of power system loads. Constant power may be reasonable for approximate static analysis when a significant proportion of the load is motors [11]. However, employing a static model for constant MVA loads can lead to erroneous and, often, misleading results [5]. Large motors can also be modeled by an exponential model in which the real power and the reactive power depend on voltage and frequency variation [11]. However, this model has proven not to be accurate in every case.

In this work, a new static model of the induction motor will be developed, and it will have a behavior closer to reality with respect to changes in variables of the network to which it is connected. Thus, a fourth-order algebraic equation system will be solved so as to obtain the motor slip and, from there, the reactive power consumed. To represent its behavior, a plotting method will be used, also proposed in this work. The method relates the power of the motor, the terminal voltage and the slip. This plotting method called non-conventional PV curves will be used in a case study. For the development of this model, data of the steady-state equivalent circuit of the motor is needed.

2. Static model of the induction motor

The static model of the induction motor proposed in this work can be used for any power electric system in which part of the demand consists in induction motors. However, in order to simplify the development of this topic, the work will be based on a small electric system, as shown in figure 1.

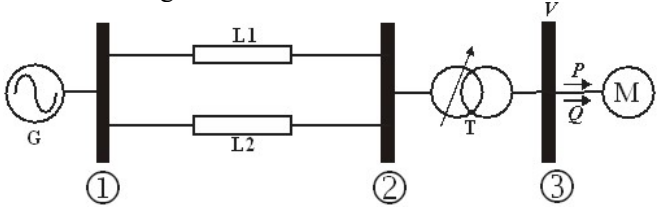

Figure 1. Small Power Systems

The synchronous generator G feeds a motor load M via two lines of transmission L1 and L2, and a transformer T. V is the terminal voltage of the motor, while P and Q are the active and the reactive power consumed by the motor. By calculating a conventional power flow (CPF), the base case for this electric system can be obtained. The data of P and Q are input data in the study of power flow, while the value of V corresponds to the output data.

To calculate the slip in those conditions, it is necessary to know the steady-state equivalent circuit parameters of the motor shown in figure 2.

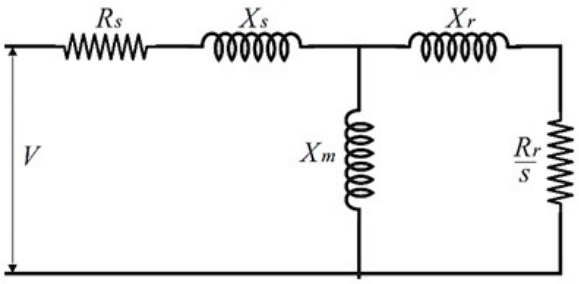

Figure 2. Induction motor equivalent circuit

Where:
R_s = Stator winding resistance
X_s = Inductive reactance of the stator winding
X_m = Magnetizing reactance
X_r = Rotor Reactance
R_r = Rotor Resistance
s = slip

With these parameters, the motor slip can be calculated by solving the following system of equations:

$$0 = a + b\,s + c\,s^2 + d\,s^3 + e\,s^4 \quad (1)$$

where the coefficients are the following:

$$a = P\,R_s^2 + P\,X_m^2 + 2P\,X_m X_s + P\,X_s^2 - R_s\,V^2 \quad (2)$$

$$b = 2P\,R_s\,X_m^2 - X_m^2\,V^2 \quad (3)$$

$$c = P\,X_m^4 + 2P\,R_s^2(X_r + X_m)^2 + 2P\,X_m^2 X_r(X_r + X_m) + 2P\,X_m X_s(X_r + X_m)^2 + 2P\,X_m X_r X_s(X_r + X_m) + 2P\,X_s^2(X_r + X_m)^2 - 2V^2 R_s\,(X_r + X_m)^2 \quad (4)$$

$$d = 2PR_s\,X_m^2(X_r + X_m)^2 - V^2 X_m^2(X_r + X_m)^2 \quad (5)$$

$$e = P\,(R_s^2(X_r + X_m)^4 + X_m^2\,X_r^2(X_r + X_m)^2 + 2\,X_m\,X_r\,X_s(X_r + X_m)^3 + X_s^2(X_r + X_m)^4 - V^2 R_s\,(X_r + X_m)^4 \quad (6)$$

The values of P and V in the equations (2) to (6) are the ones obtained in the base case, which is $P = P_{bc}$ and $V = V_{bc}$., when a subscript bc will be assigned for the base case.

The solution to the system of equations (1) to (6) results in four roots. Two of them are complex conjugate roots and have no physical meaning for this problem. The other two roots represent two possible motor slip values. The highest value represents the slip for a state of unstable balance, so it must be dismissed. The lowest value represents the slip for steady-state conditions, in this case, for the base case.

The value of reactive power used as input data in power flow should be confirmed by the following equations:

$$Z_r = \frac{R_r}{s} + iX_r \quad (7)$$

$$Z_m = \left(\frac{iX_m\,Z_r}{iX_m + Z_r}\right) + R_s + i\,X_s \quad (8)$$

$$Q_{bc} = \frac{imag(Z_m)\ |V|^2}{[real(Z_m)\,]^2 + [imag(Z_m)\,]^2} \quad (9)$$

where i is the imaginary unit, Z_r is the rotor impedance, and Z_m is the motor impedance. If the value of the Q_{bc} obtained matches input data, the next step can be followed; otherwise, input data should be corrected and the base case should be recalculated.

In sum, for the base case, the following variables that correspond to each motor load: P_{bc}, Q_{bc}, V_{bc}, and motor slip, s_{bc} are known.

Now, a fault will be produced on the electric system under study, causing a voltage drop in the network and at the motor terminals. This will produce changes in the active and the reactive power consumed. However, these changes in power will not be reflected in the power flow output applied to the faulty network. This must be corrected by the following equation:

$$P_{pf} = P_{bc}\,V_{pf}^{0.01} \quad (10)$$

where:
P_{pf} = Active power of the post-fault motor
V_{pf} = Terminal voltage of the post-fault motor

This empirical equation reflects the variations in active power of the induction motor when facing voltage variations.

With V_{pf} and P_{pf} values of each load, the new post-fault slip value s_{pf} can be calculated by equations 1 to 6. Then, the new value of reactive power consumed Q_{pf} can be calculated by equations 7 to 9. These equations should be inserted in the iterative process of the CPF, according to the flowchart that outlines the previously described process in figure 3. This modification in the CPF can be

part of a group of additional changes that model other network devices more in detail, so as to achieve a more realistic behavior in the face of problems with voltage stability when using static calculation techniques.

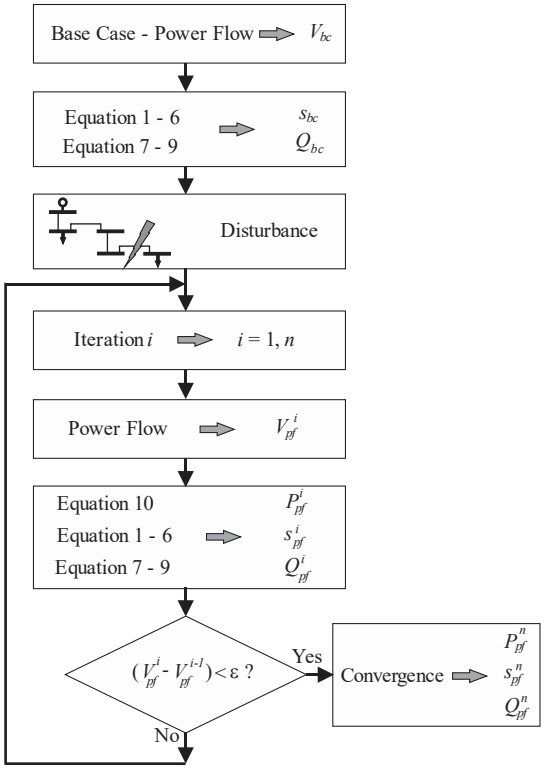

Fig. 3. Flowchart

3. Case study

The electric system shown in figure 4 will be analyzed as case study. The generator feeds a large induction motor via two transmission lines and one transformer. Furthermore, a capacitor bank is also connected to the load bus. The voltage and impedance values are indicated per unit.

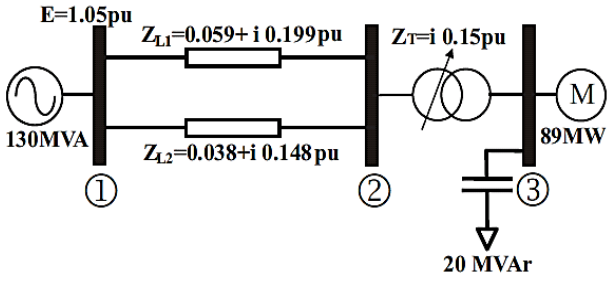

Figure 4. Small power systems

Figure 5 shows the equivalent circuit and the motor parameters expressed per unit.

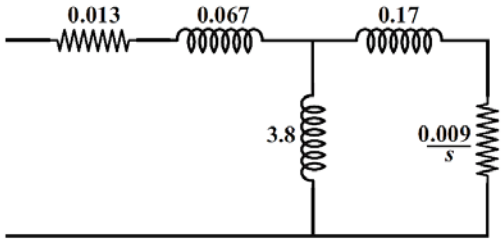

Figure 5. Induction motor parameters

The solution to the base case yields the following results related to the induction motor:

V_{3bc} = Terminal voltage = 1∠–11º
s_{bc} = Motor slip = 0.0088
P_{mbc} = Active power consumed = 89 MW
Q_{mbc} = Reactive power consumed = 45.5 MVAr

A perturbation consisting in disconnecting one of the transmission lines according to the following cases will be applied:

- Case 1: Disconnection without fault of transmission line Z_{L1}
- Case 2: Disconnection without fault of transmission line Z_{L2}

In order to solve the case study proposed, three different calculation techniques will be applied to compare the results obtained, according to the following detail:

a) Conventional static technique, in which the motor is modeled as a constant power load. This technique will be represented by PV curves that relate terminal voltage and the load active power with the factor of constant power.

b) Static technique proposed in this work: This technique will be represented by non-conventional PV curves that relate terminal voltage and the active power consumed by the motor when its slip varies.

c) Conventional dynamic technique, in which the motor is modeled by differential equations. The output curves show terminal voltage variations and the active power consumed versus time. Therefore, the program PSS/E V 32 by Siemens will be used.

3.1 Case 1.

In figure 6, conventional PV curves, load curves at constant pre-fault and post-fault impedance, and the line of *Pcte* = 0.89 pu are shown. The intersection of the pre-fault PV curves, *pre-fault Zcte* and the line of *Pcte* occurs at point A, which indicates a steady state point for the base case. After perturbation, the values move according

to the constant impedance curve until they intersect the post-fault PV curve at point B. Then, the power tends to recover its pre-fault values until it converges at point C. Here, a new steady state point is set at the following values:

$|V_{3pf}|$ = Terminal voltage = 0.9324 pu
P_{mpf} = Active power consumed = 0.89 pu

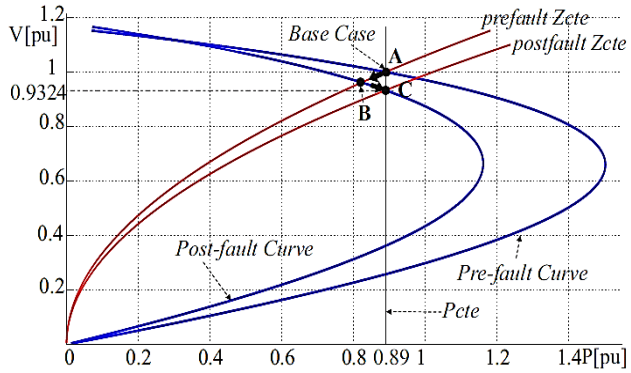

Figure 6. Case 1 conventional PV curve

Figure 7 plots the static technique proposed in this work. Pre-fault and post-fault non-conventional PV curves, constant slip curves, and the motor active power vs terminal voltage curve, obtained by equation 10, can be identified. Point A is the intersection of the pre-fault non-conventional PV curve, the constant slip curve of the base case, and the active power curve of equation 10. After perturbation, the values move according to the constant slip curve until they intersect the post-fault non-conventional PV curve at point B. Then, the power tends to recover its pre-fault values until it converges at point C. Here, a new steady state point is set at the following values:

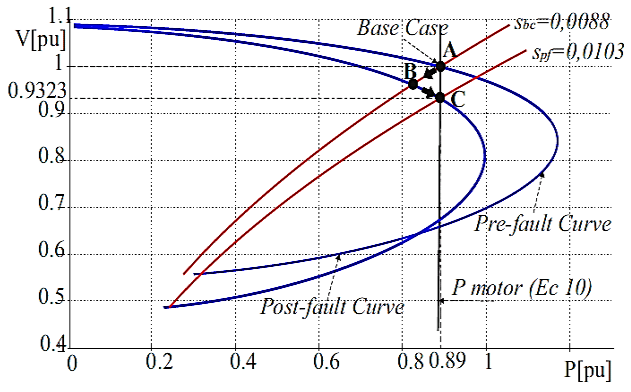

Figure 7. Case 1 non-conventional PV curve

$|V_{3pf}|$ = Terminal voltage = 0.9323 pu
P_{mpf} = Active power consumed = 0.89 pu
s_{pf} = Motor slip = 0.0103

Figure 8 plots the conventional dynamic technique. The output curves indicate the behavior of the terminal voltage and the active power consumed by the motor throughout time. Perturbation is applied to 1 s time. After some oscillations, the power and motor voltage are stabilized at the following values:

$|V_{3pf}|$ = Terminal voltage = 0.9323 pu
P_{mpf} = Active power consumed = 0.89 pu

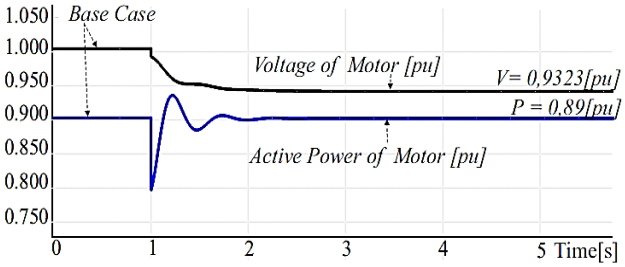

Figure 8. Case 1 Conventional dynamics

As it can be observed, all techniques applied lead to the conclusion that the system is stable, and that the voltage and power values are similar.

3.2 Case 2.

Figure 9 plots the conventional PV curves, load curves at constant pre-fault and post-fault impedance, and the line of $Pcte$ = 0.89 pu are shown. The intersection of the pre-fault PV curves, pre-fault Zcte and the line of Pcte occurs at point A, which indicates a steady state point for the base case. After perturbation, the values move according to the constant impedance curve until they intersect the post-fault PV curve at point B. Then, the power tends to recover its pre-fault values until it converges at point C. Here, a new steady state point is set at the following values:

$|V_{3pf}|$ = Terminal voltage = 0.827 pu
P_{mpf} = Active power consumed = 0.89 pu

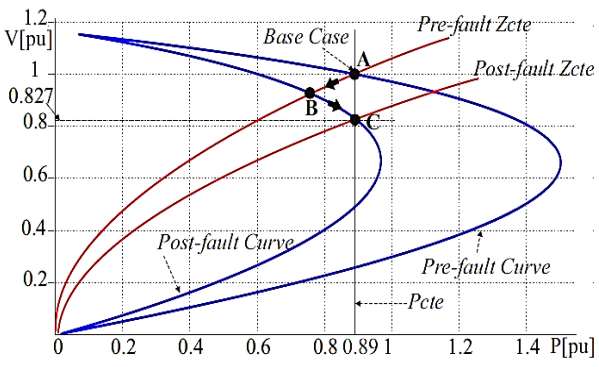

Figure 9. Case 2 conventional PV curve

Figure 10 plots the static technique proposed in this work. As in case 1, pre-fault and post-fault non-conventional PV curves, the constant slip curve, and the motor active power vs terminal voltage curve, obtained by equation 10, can be identified. Point A is the intersection of the pre-fault non-conventional PV curve, the constant slip curve of the base case, and the active power curve of equation 10. After perturbation, the values move according to the constant slip curve until they intersect the post-fault non-conventional PV curve at point B. Then, the power tends to recover its pre-fault values, but it does not converge, as there is no intersection of the post-fault curve and the *Pmotor* curve. Thus, the system loses voltage stability under these conditions.

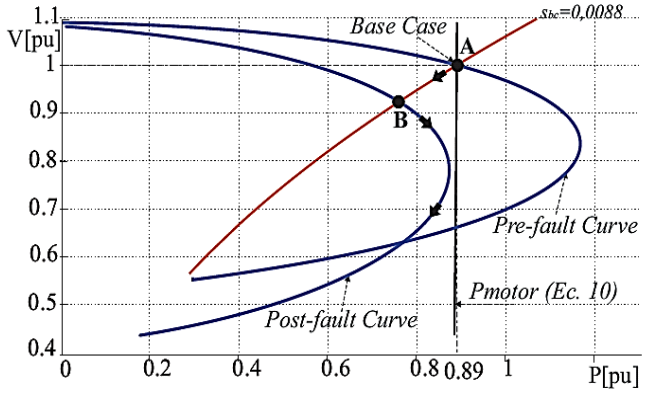

Figure 10. Case 2 non-conventional PV curve

Figure 11 plots the conventional dynamic technique for this case. The output curves indicate the behavior of the terminal voltage and the active power consumed by the motor throughout time. Perturbation is applied to 1 s time. It can be observed that, for this case, system voltage stability is lost because values collapse to unacceptable values.

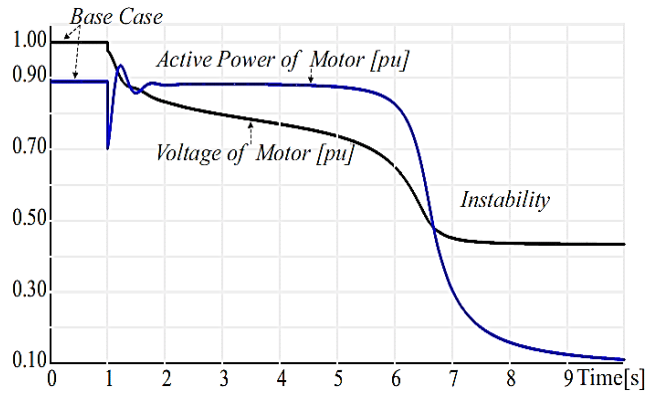

Figure 11. Case 2 Conventional dynamics

In table 1, the results obtained for voltage and post-fault active power for cases 1 and 2 are summarized.

Table 1

Case		PV Curve		Dynamic [pu]
		Conven-tional [pu]	Non-Conventional [pu]	
1	V_{3pf}	0.9324	0.9323	0.9323
	P_{mpf}	0.89	0.89	0.89
2	V_{3pf}	0.827	Non-convergence	Instability
	P_{mpf}	0.89	Non-convergence	Instability

4. Conclusions

We have shown a static model of induction motor which can be applied to any study of static voltage stability in order to improve the accuracy of results. The model proposed indicates a substantial improvement versus the conventional model, as it achieves results highly comparable to the ones obtained by dynamic techniques of calculation.

5. References

1 Ping Ju, Chuan, Qin, Feng Wu, Huiling Xie, Yan Ning: *Load modeling for wide area power system*. Electrical Power and Energy Systems 33 (2011) 909-917.

2 Hao Wu, Ian Dobson: *Cascading Stall of Many Induction*. IEEE Transactions on power systems, vol. 27, Nº4, November 2012.

3 González, E., Guizar, J. G.: *The Effect of Induction Motor Modeling in the context of voltage sensitive: combined loads*. IEEE Latin America Transactions, vol. 10, Nº. 4, June 2012

4 Mahmud, M.A., Hossain, M. J., Pota H., R.: *Effects of large dynamic loads on power system stability*. Electrical Power and Energy Systems 44 (2013) 357-363.

5 Yinhong Li, Hsiao-Dong Chiang, Byoung-Kon Choi, Yung-Tien Chen, Der-Hua Huang, Mark G. Lauby: *Load models for modeling dynamic behaviors of reactive loads: Evaluation and comparison*. Electrical Power and Energy Systems 30 (2008) 497-503.

6 Rajive Tiwari, K. R, Niazi, Vikas Gupta: *Line collapse proximity index for prediction of voltage collapse in power systems*. Electrical Power and Energy Systems 41 (2012) 105-111.

7 Mostafa Eidiani: *A reliable and efficient method for assessing voltage stability in transmission and distribution networks*. Electrical Power and Energy Systems 33 (2011) 453-456.

8 Borghettia, A., Caldonb, R., Nuccia. C. A.: *Generic dynamic load models in long-term voltage stability studies*. Electrical Power and Energy Systems 22 (2000) 291-301

9 Jiajia Song, Cotilla-Sanchez, Eduardo, Brekken, Ted K. A.: *Load Modeling Methodologies for Cascading Outage Simulation Considering Power System Stability*. 2013 1st IEEE Conference on Technologies for Sustainability (SusTech). 78-85.
10 Kundur, P.: *Power System Stability and Control*. McGraw-Hill.1994.
Taylor, C.: *Power System Voltage Stability*. McGraw-Hill.1994.
11 Machowski; J. Bialek; J Bumby. .J.:*Power System Dynamics Stability and Control*. Second Edition. Wiley, 2008.
12 Siemens, PSS/E 32.0.5, Manual
13 IEEE/GIGRE Joint Task Force on Stability Terms and Definitions. *Definition and Classification of Power System Stability*, IEEE Transaction of Power Systems, Vol 19, N.º 2, pp 1387-1401, May 2004.

6 Author names and affiliations

Luis Aromataris. Mechanical Electrical Engineer and Doctor of Engineering. Professor at the Electricity and Electronics Department of the School of Engineering at the National University of Rio Cuarto. Member of the Executive Committee of the Electric Power System Analysis Group (GASEP).

Fabian Rinaudo. Electrical Engineer. Candidate for Doctor of Engineering. Adscript Professor at the Electricity and Electronics Department of the School of Engineering at the National University of Rio Cuarto. Member of the Electric Power System Analysis Group (GASEP).

Juan Alemany. Electrical Engineer and Doctor of Engineering. Professor at the Electricity and Electronics Department of the School of Engineering at the National University of Rio Cuarto. Member of the Electric Power System Analysis Group (GASEP).

Marcos Galetto. Electrical Engineer. Professor at the Electricity and Electronics Department of the School of Engineering at the National University of Rio Cuarto. Member Electric Power System Analysis Group (GASEP).